

Pathogenic prions deviate PrPC signaling in neuronal cells and impair A-beta clearance

E Pradines, J Hernandez-Rapp, A Villa-Diaz, C Dakowski, H Ardila-Osorio, S Haik, S Schneider, J-M Launay, O Kellermann, J-M Torres, et al.

▶ **To cite this version:**

E Pradines, J Hernandez-Rapp, A Villa-Diaz, C Dakowski, H Ardila-Osorio, et al.. Pathogenic prions deviate PrPC signaling in neuronal cells and impair A-beta clearance. Cell Death and Disease, 2013, 4, pp.e456. 10.1038/cddis.2012.195 . hal-01548467v2

HAL Id: hal-01548467

https://hal.sorbonne-universite.fr/hal-01548467v2

Submitted on 27 Jun 2017

HAL is a multi-disciplinary open access archive for the deposit and dissemination of scientific research documents, whether they are published or not. The documents may come from teaching and research institutions in France or abroad, or from public or private research centers.

L'archive ouverte pluridisciplinaire **HAL**, est destinée au dépôt et à la diffusion de documents scientifiques de niveau recherche, publiés ou non, émanant des établissements d'enseignement et de recherche français ou étrangers, des laboratoires publics ou privés.



Distributed under a Creative Commons Attribution| 4.0 International License

Citation: Cell Death and Disease (2013) 4, e456; doi:10.1038/cddis.2012.195
© 2013 Macmillan Publishers Limited All rights reserved 2041-4889/13
www.nature.com/cddis

Pathogenic prions deviate PrP^C signaling in neuronal cells and impair A-beta clearance

E Pradines[1,2,10], J Hernandez-Rapp[1,2,3,10], A Villa-Diaz[4], C Dakowski[1,2], H Ardila-Osorio[1,2], S Haik[5,6,7], B Schneider[1,2], J-M Launay[8,9], O Kellermann[1,2], J-M Torres[4] and S Mouillet-Richard*[,1,2]

The subversion of the normal function exerted by the cellular prion protein (PrP^C) in neurons by pathogenic prions is assumed to have a central role in the pathogenesis of transmissible spongiform encephalopathies. Using two murine models of prion infection, the 1C11 neuronal cell line and neurospheres, we document that prion infection is associated with the constitutive activation of signaling targets normally coupled with PrP^C, including the Fyn kinase, the mitogen-associated protein kinases ERK1/2 and the CREB transcription factor. PrP^C-dependent signaling overactivation in infected cells is associated with the recruitment of p38 and JNK stress-associated kinases. Downstream from CREB, prion-infected cells exhibit reduced activity of the matrix metalloprotease (MMP)-9. As MMP-9 catalyzes the degradation of the amyloid A-beta peptide, the decrease in MMP-9 activity in prion-infected cells causes a significant impairment of the clearance of A-beta, leading to its accumulation. By exploiting two 1C11-infected clones accumulating high or moderate levels of prions, we show that the prion-induced changes are correlated with the level of infectivity. Of note, a dose-dependent increase in A-beta levels was also found in the cerebrospinal fluid of mice inoculated with these infected clones. By demonstrating that pathogenic prions trigger increases in A-beta levels through the deviation of PrP^C signaling, our data argue that A-beta may exacerbate prion-induced toxicity.

Cell Death and Disease (2013) **4,** e456; doi:10.1038/cddis.2012.195; published online 10 January 2013
Subject Category: Neuroscience

Transmissible spongiform encephalopathies (TSEs), are a group of fatal neurodegenerative disorders, including Creutzfeldt–Jakob disease (CJD) in humans, bovine spongiform encephalopathy and scrapie in animals. A central feature of these diseases is the accumulation of an infectious and neurotoxic protein, named disease-associated scrapie prion protein (PrP^{Sc}). PrP^{Sc} is the pathogenic isoform of a host-encoded protein, the cellular prion protein (PrP) (PrP^C).[1] Although it is well established that the conversion of PrP^C into PrP^{Sc} lies at the root of TSEs, the mechanisms through which PrP^{Sc} exerts its toxicity remain poorly understood.

Depletion of neuronal PrP^C in scrapie-infected mice impedes TSE pathogenesis despite massive extraneuronal PrP^{Sc} accumulation.[2] Moreover, scrapie infection of transgenic mice expressing a PrP lacking its glycosylphosphatidylinositol (GPI) moiety triggers efficient prion replication without any TSE pathology.[3] Thus, the expression of GPI-anchored PrP^C at the neuronal cell surface is required for the neurotoxic action of PrP^{Sc}. TSE-associated neuronal dysfunction is actually assumed to result from alterations of PrP^C normal function induced by its conversion into PrP^{Sc}.[4] PrP-null mice, which are resistant to prion infection, do not show any sign of neurodegeneration.[5] Hence, it is unlikely that the loss of PrP^C normal function represent a critical causal event in TSE-associated neuropathogenesis. PrP^{Sc} neurotoxicity may rather involve some toxic gain of PrP^C function. This notion is supported by the development of a spontaneous neurodegenerative illness in transgenic mice overexpressing wild-type PrP^C by 5- to 10-fold.[6] Unraveling the physiological function of PrP^C in neuronal cells thus represents a major issue to decipher the cellular and molecular events leading to neurodegeneration in TSEs.[7] Answers to this question may actually have a broad significance in the field of neurodegenerative disorders because PrP^C appears to mediate the toxicity of diverse beta-sheet rich oligomers, including the beta-amyloid peptide A-beta.[8]

Over the last decade, much attention has been devoted to the involvement of PrP^C in signal transduction.[7,9] By exploiting the 1C11 neuroectodermal cell line, which can differentiate into either serotonergic ($1C11^{5\text{-}HT}$) or noradrenergic ($1C11^{NE}$)

[1]Cellules Souches, Signalisation et Prions, INSERM UMR-S747, 75006, Paris, France; [2]Université Paris Descartes, Sorbonne Paris Cité, UMR-S747, 75006, Paris, France; [3]Université Paris Sud 11, ED419 Biosigne, 91400 Orsay, France; [4]Centro de Investigación en Sanidad Animal-INIA, Madrid, Spain; [5]Université Pierre et Marie Curie-Paris 6, Centre de Recherche de l'Institut du Cerveau et de la Moelle épinière (CRICM), UMR-S975, Equipe 'Alzheimer's and Prion Diseases', 75013, Paris, France; [6]INSERM, UMR-S975, 75013, Paris, France; [7]CNRS UMR 7225 75013, Paris, France; [8]AP-HP Service de Biochimie, Fondation FondaMental, INSERM U942 Hôpital Lariboisière, 75010, Paris, France and [9]Pharma Research Department, F Hoffmann-La-Roche Ltd, CH-4070 Basel, Switzerland
*Corresponding author: S Mouillet-Richard, INSERM UMR-S747, Université Paris Descartes, 45 rue des Saints Pères, Paris, 75006, France. Tel: +33 1 42 86 20 67; Fax: +33 1 42 86 40 68; E-mail: sophie.mouillet-richard@parisdescartes.fr
[10]These two authors contributed equally to this work.
Keywords: prion infection; A-beta; signal transduction; MMP-9
Abbreviations: βDG, beta-dystroglycan; CCA, cyclohexane carboxylic acid; CJD, Creutzfeldt–Jakob disease; CSF, cerebrospinal fluid; dbcAMP, dibutyryl cyclic AMP; ECM, extracellular matrix; GPI, glycosylphosphatidylinositol; MAPK, mitogen-associated protein kinase; MMP, matrix metalloprotease; PrP, prion protein; PrP^C, cellular prion protein; PrP^{Sc}, disease-associated scrapie prion protein; ROS, reactive oxygen species; SAPK, stress-associated protein kinase; TSE, transmissible spongiform encephalopathy
Received 31.7.12; revised 23.11.12; accepted 28.11.12; Edited by A Verkhratsky

neuronal cells,[10] we have unraveled some cell signaling events imparted by PrP^{C}.[11–13] In differentiated cells, PrP^{C} has the ability to mobilize a caveolin-Fyn platform on neurites upon antibody-mediated ligation.[11] Signaling effectors downstream from Fyn include the reactive oxygen species (ROS)-generating enzyme NADPH oxidase, the mitogen-associated protein kinases (MAPKs) ERK1/2 and the transcription factors CREB, Egr-1 and c-Fos.[12,13] Besides, PrP^{C} contributes to extracellular matrix (ECM) remodeling by regulating the expression of the matrix metalloprotease (MMP)-9 and, consequently, limiting the cleavage of beta-dystroglycan (βDG),[12] which links the ECM to the cytoskeleton. The identification of various targets within PrP^{C}-mediated cascades provides molecular readouts to probe PrP^{Sc} action. 1C11 cells may help to assess the impact of pathogenic prions on PrP^{C} normal function because they support the replication of various prion strains. Chronically infected 1C11 cells retain the ability to implement a bioaminergic neuronal differentiation program upon induction.[14] However, the differentiated progenies of infected cells show drastic decrease in neurotransmitter-associated functions and produce bioamine-derived oxidized species.[14]

Here, we examined the status of PrP^{C} signaling targets under prion infection. Our approach combines the use of two *in vitro* models, the 1C11 cell line and neurosphere cultures. We first exploited two 1C11-derived clones infected with Fukuoka prions with high (1C11Fk6) or moderate (1C11Fk7) PrP^{Sc} levels[14] to assess dose-dependent effects of prion infection. The second paradigm relies on murine neurospheres derived from whole brains of wild-type and PrP-null embryos (ED14).[15] After exposure to different prion strains, wild-type neurospheres efficiently replicate prions when induced to differentiate, while not accumulating PrP^{Sc} in their undifferentiated state.[15] We provide evidence that prion infection promotes an overactivation of PrP^{C} signaling targets in the differentiated progenies of both 1C11 cells and neurospheres. We further show that the cascade of PrP^{Sc}-mediated events culminates with a decreased clearance of A-beta in 1C11Fk-infected cells, and that A-beta levels are increased in the cerebrospinal fluid (CSF) of prion-infected mice.

Results

PrP^{Sc} corrupts the 'Fyn–ERK–CREB–Egr-1' cascade in prion-infected 1C11Fk$^{5\text{-HT}}$ neuronal cells. The status of PrP^{C} signaling targets was first examined in the serotonergic neuronal derivatives of 1C11Fk-infected cells (1C11Fk$^{5\text{-HT}}$). At a proximal level, the detection of activated Src kinase proteins, including Fyn, was performed with antibodies against phospho-Tyr418 Src. PrP^{Sc} accumulation (Figure 1a) was associated with an increase in Src kinases activation, which was more prominent in the highly infectious 1C11Fk6$^{5\text{-HT}}$ cells ($\times$2.9) than in the less infectious 1C11Fk7$^{5\text{-HT}}$ cells ($\times$2.1; Figure 1b). Infection also triggered a significant rise in the phosphorylation of ERK1/2 on Thr185/Tyr187 ($\times$1.8) and CREB on Ser133 ($\times$2) in

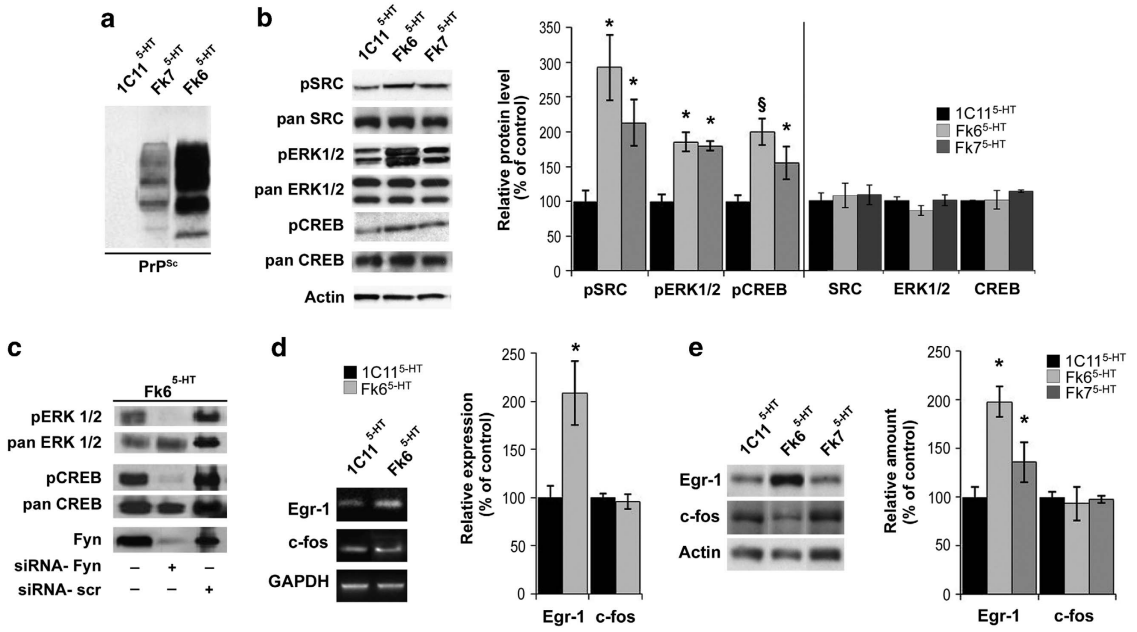


Figure 1 PrP^{Sc} constitutively activates the Fyn–ERK–CREB–Egr1 cascade in 1C11Fk$^{5\text{-HT}}$-infected cells. (**a**) Protein extracts from 1C11$^{5\text{-HT}}$, 1C11Fk6$^{5\text{-HT}}$ and 1C11Fk7$^{5\text{-HT}}$ were digested with proteinase K and subjected to western blot to detect PrP^{Sc}. (**b**) Immunoblots and quantification histograms of 1C11$^{5\text{-HT}}$, 1C11Fk6$^{5\text{-HT}}$ and 1C11Fk7$^{5\text{-HT}}$ cell lysates, using antibodies against src [pY418], pan src, ERK [pT185/pY187], pan ERK1/2, CREB [pS133] and pan CREB. Antibody against actin was used as loading control (**c**) 1C11Fk6$^{5\text{-HT}}$ cells were transfected with a siRNA targeted against Fyn or a control siRNA. The phosphorylation levels of ERK and CREB were compared with the total form of these proteins by immunoblotting. (**d**) The mRNA levels of Egr-1 and c-fos were measured by RT-PCR in 1C11Fk6$^{5\text{-HT}}$ cells *versus* 1C11$^{5\text{-HT}}$ cells. GAPDH was used as an internal control for normalization. (**e**) Cells lysates from 1C11$^{5\text{-HT}}$, 1C11Fk6$^{5\text{-HT}}$ and 1C11Fk7$^{5\text{-HT}}$ were immunoblotted with antibodies targeting Egr-1 and c-fos. All data shown are representative of a set of $n = 3$ experiments. Results are expressed as means $\pm$ S.E.M of three independent experiments. $^{*}P \leq 0.05$, $^{\S}P \leq 0.005$ *versus* control, (Student's *t*-test)

1C11Fk6$^{5\text{-HT}}$ cells (Figure 1b). Both changes were also observed in 1C11Fk7$^{5\text{-HT}}$ cells, albeit at a milder level (Figure 1b). The global levels of src, ERK1/2 and CREB proteins were, however, unaffected by prion infection (Figure 1b).

Of note, siRNA-mediated knockdown of Fyn in 1C11Fk6$^{5\text{-HT}}$ completely abolished the phosphorylation of ERK1/2 and CREB (Figure 1c), indicating that, in 1C11Fk$^{5\text{-HT}}$ cells, the constitutive activation of these two signaling effectors by pathogenic prions is fully dependent on the recruitment of the Fyn kinase.

In 1C11 cells, PrP^{C} instructs the expression of the two immediate-early genes Egr-1 and c-fos.[12] In 1C11Fk6$^{5\text{-HT}}$-infected cells, we observed a twofold increase in Egr-1 mRNA and protein levels versus non-infected 1C11$^{5\text{-HT}}$ cells (Figure 1d and e). In the less infected 1C11Fk7$^{5\text{-HT}}$ cells, the increase in Egr-1 protein levels reached 1.4-fold that of uninfected 1C11$^{5\text{-HT}}$ cells. In contrast, PrP^{Sc} accumulation did not trigger any significant change in c-fos transcript or protein levels in 1C11Fk$^{5\text{-HT}}$ cells (Figure 1d and e). These discordant regulations of c-fos and Egr-1 may be accounted for by distinct transcriptional regulatory mechanisms of the two genes.[16]

At this stage, our data provide evidence for a dose-dependent effect of PrP^{Sc} on the basal activation levels of Src kinases, ERK1/2, CREB and Egr-1. The full control of Fyn on the activation of ERK and CREB in 1C11Fk6$^{5\text{-HT}}$ cells argues for a constitutive recruitment of the caveolin-Fyn platform by PrP^{Sc}, which imparts neurospecificity to PrP^{C} signaling.[7,11]

PrP^{Sc} deviates PrP^{C} signaling in infected neurospheres. We then sought to extend these observations to other prion-infected neuronal cells. We designed an experimental strategy based on cultured neurospheres derived from wild-type or PrP-null mice (Figure 2a), which were exposed to a 22L prion inoculum during the first 24 h of differentiation, as in Herva *et al.*[15] PrP^{Sc} levels increased with time in cells derived from wild-type mice, whereas no PrP^{Sc} was detectable in PrP-null cells (Figure 2b), confirming that only wild-type cells can replicate prions. Cell extracts were collected at 5 days post-infection (d.p.i.), when neurospheres are clearly differentiated, as inferred by the expression of neuronal markers (Figure 2c and[15]). PrP^{Sc} accumulation induced a significant increase in the phosphorylation of Src kinases ($\times$ 1.9), ERK1/2 ($\times$ 3.6), CREB ($\times$ 3) and in the level of the Egr-1 protein ($\times$ 1.5) in infected neurospheres derived from wild-type mouse (Figure 2d). As with 1C11$^{5\text{-HT}}$ cells, prion infection did not alter the total levels of src, ERK1/2 and CREB proteins (Supplementary Figure S1). Besides, the status of these effectors in PrP$^{-/-}$-derived neurospheres was insensitive to the exposure to 22L prions (Figure 2d). Thus, prion replication in differentiated PrP^{C}-expressing neurospheres promotes the constitutive recruitment of cell signaling intermediates associated with PrP^{C}-dependent pathways.

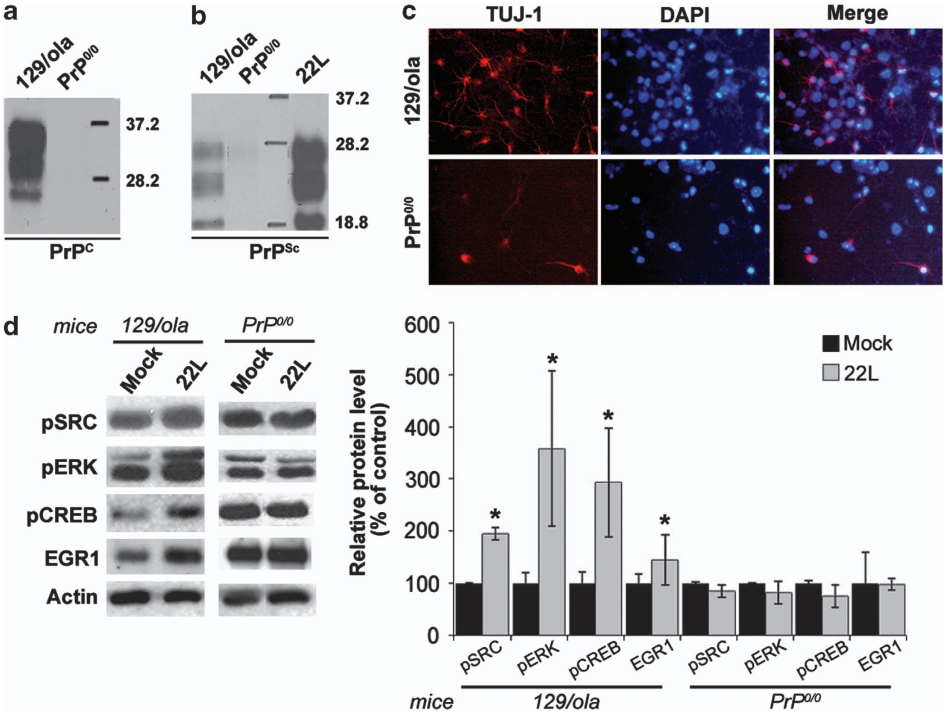


Figure 2 Constitutive activation of the Fyn–ERK–CREB–Egr1 cascade in prion-infected differentiated neurospheres. (**a**) PrP^{C} expression in neurospheres obtained from 129/ola WT (lane 1) or PrP-null mice (lane 2) as determined by western blot. (**b**) Protein extracts from neurospheres derived from 129/ola WT (lane 1) or PrP-null mice (lane 2), inoculated with 22L mouse brain homogenate were digested with proteinase K and subjected to western blot to detect PrP^{Sc}. Lane 3 corresponds to the 22L inoculum. (**c**) Neurosphere cultures derived from 129/ola or PrP$^{0/0}$ mice stained after 5 days of differentiation with the neuron-specific class III b-tubulin TUJ-1 (red) and DAPI (blue). (**d**) Cell lysates from mock-infected or 22L-infected neurospheres derived from 129/ola WT or PrP-null mice were immunoblotted with antibodies against src [pY418], ERK [pT185/pY187] and CREB [pS133] and Egr1. Results are expressed as means $\pm$ S.E.M of three independent experiments. $^{*}P \leq 0.05$ *versus* control (Student's *t*-test)

PrP^{Sc} replication promotes the recruitment of the stress-sensitive p38 and JNK1/2 SAPKs. Our previous work demonstrated that exposure of 1C11$^{5\text{-HT}}$ cells to the neurotoxic prion peptide 106–126 triggers long-lasting activation of JNK1/2 and p38 stress-associated protein kinases (SAPKs) as a consequence of NADPH oxidase-dependent excessive ROS synthesis.[17] Besides, PrP^{Sc} accumulation promotes the production of oxidized derivatives of bioamines in 1C11Fk$^{5\text{-HT}}$ cells, which mirror oxidative stress conditions.[14] We thus probed if pathogenic prions could lead to the phosphorylation of SAPKs. The phosphorylation levels of JNK1/2 and p38 were 2- to 2.5-fold higher in 1C11Fk6$^{5\text{-HT}}$ cells than in 1C11$^{5\text{-HT}}$-uninfected cells (Figure 3a). In 1C11Fk7$^{5\text{-HT}}$ cells, we detected only a faint increase in phospho-p38 (Figure 3a). Increased levels of phospho-JNK and phospho-p38 were also observed in infected neurospheres derived from wild-type mouse but not in their PrP$^{-/-}$ counterparts (Figure 3b).

Upon siRNA-mediated silencing of Fyn, the levels of phospho-JNK and phospho-p38 in 1C11Fk6$^{5\text{-HT}}$-infected cells did not exceed those measured in their non-infected counterparts (Figure 3c). In the less infected 1C11Fk7$^{5\text{-HT}}$ cells, the level of phospho-JNK was similar to that of uninfected cells (Figure 3a), and reduced under Fyn knockdown (Figure 3c). This suggests the occurrence of compensatory mechanisms to prevent excessive JNK activation in cells with moderate (1C11Fk7$^{5\text{-HT}}$) – but not high (1C11Fk6$^{5\text{-HT}}$) – PrP^{Sc} levels. Finally, we sought to cancel the production of ROS by using a siRNA against the p22phox subunit of NADPH oxidase. Blocking p22phox reversed the phosphorylation of JNK1/2 and p38 in 1C11Fk$^{5\text{-HT}}$-infected cells (Figure 3d). These observations indicate that the recruitment

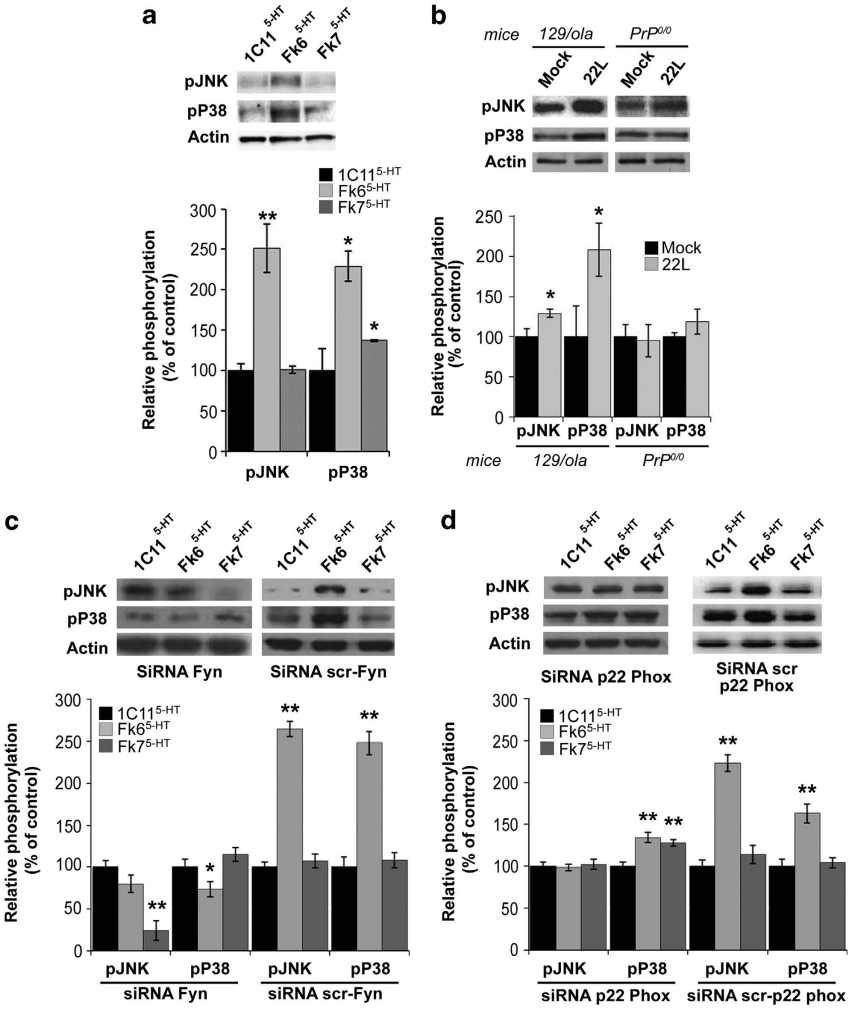


Figure 3 Prion infection induces the phosphorylation of stress-sensitive MAPKs. (**a**) The phosphorylation levels of JNK [pT183/pY185] and p38 [pT180/pY182] were analyzed by western blot in lysates from 1C11$^{5\text{-HT}}$, 1C11Fk6$^{5\text{-HT}}$ and 1C11Fk7$^{5\text{-HT}}$ cells. (**b**) Cell lysates from neurospheres derived from 129/ola or Prnp$^{0/0}$ mice, and either mock-infected or infected with 22L prions were immunoblotted with antibodies targeting JNK [pT183/pY185] and p38 [pT180/pY182]. (**c**) 1C11$^{5\text{-HT}}$, 1C11Fk6$^{5\text{-HT}}$ and 1C11Fk7$^{5\text{-HT}}$ cells were transfected with a siRNA targeted against the Fyn kinase or a control siRNA. Cell lysates were immunoblotted using antibodies against JNK [pT183/pY185] and p38 [pT180/pY182]. (**d**) The phosphorylation levels of JNK [pT183/pY185] and p38 [pT180/pY182] were analyzed by western blot in lysates from 1C11$^{5\text{-HT}}$, 1C11Fk6$^{5\text{-HT}}$ and 1C11Fk7$^{5\text{-HT}}$ cells transfected with a siRNA against the p22Phox subunit of NADPH oxydase or a control siRNA. Results are expressed as means ± S.E.M of three independent experiments. *$P \leq 0.05$ and **$P \leq 0.01$ *versus* control, (Student's *t*-test)

of a stress-related cascade by prions relates to an excessive ROS production by the NADPH oxidase, downstream from Fyn.

Prion replication interferes with MMP-9 activity and inhibits βDG cleavage. We previously documented a decrease in MMP-9 mRNA level following antibody-mediated ligation of PrP^{C} in neuronal 1C11$^{5\text{-HT}}$ cells, downstream from CREB.[12] By decreasing MMP-9 activity, PrP^{C} signaling prevents the MMP-9-mediated cleavage of βDG.[12] If PrP^{Sc} deviates the PrP^{C}-dependent signaling cascades, then we anticipate a reduction of MMP-9 expression in infected cells. Indeed, we measured a 38% reduction in the mRNA levels of MMP-9 in 1C11Fk6$^{5\text{-HT}}$ cells compared with 1C11$^{5\text{-HT}}$ cells (Figure 4a). This downregulation of MMP-9 transcription induced by PrP^{Sc} accumulation correlated with a significant decrease in the activity of the metalloproteinase that was more pronounced in 1C11Fk6$^{5\text{-HT}}$ (88%) than in 1C11Fk7$^{5\text{-HT}}$ (67%) cells (Figure 4b and Supplementary Figure S2). The reduction in MMP-9 activity relates to a constitutive recruitment of the caveolin-Fyn platform by prions because blockade of Fyn through siRNA allowed to restore MMP-9 activity in 1C11Fk6$^{5\text{-HT}}$-infected cells (Figure 4c).

We next examined the outcome of the PrP^{Sc}-induced downregulation of MMP-9 activity, using βDG cleavage as a readout. As expected from the decrease in MMP-9 activity, βDG from 1C11Fk6$^{5\text{-HT}}$ was mostly detected as the 43-kDa uncleaved species. The ratio of cleaved βDG *versus* total βDG in 1C11Fk6$^{5\text{-HT}}$-infected cells was reduced by nearly 35% as compared with uninfected 1C11$^{5\text{-HT}}$ cells (Figure 4d). The decrease was only 23% in 1C11Fk7$^{5\text{-HT}}$ cells, again highlighting a dose-dependent effect of PrP^{Sc}. In line with the above results, the ratio cleaved βDG/total βDG returned to the control 1C11$^{5\text{-HT}}$ level when Fyn was silenced in 1C11Fk$^{5\text{-HT}}$ cells (Figure 4d).

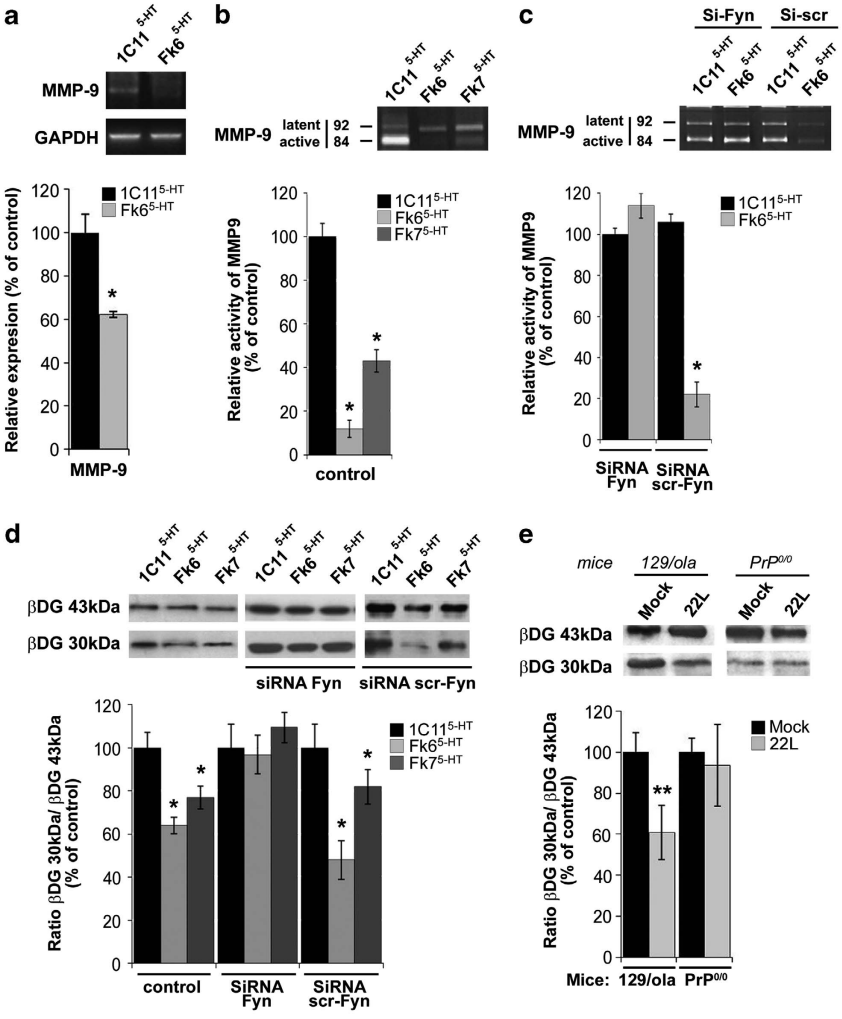


Figure 4 Prion infection decreases MMP-9 expression and activity and βDG cleavage. (**a**) The mRNA levels of MMP-9 were determined by RT-PCR, and normalized to GAPDH mRNA expression. (**b**) MMP-9 activity was measured by zymography in 1C11$^{5\text{-HT}}$, 1C11Fk6$^{5\text{-HT}}$ and 1C11Fk7$^{5\text{-HT}}$ cells. (**c**) The contribution of the Fyn kinase to the alteration of MMP-9 activity was assessed through cell transfection with a siRNA targeting Fyn or a control siRNA. (**d**) 1C11$^{5\text{-HT}}$, 1C11Fk6$^{5\text{-HT}}$ and 1C11Fk7$^{5\text{-HT}}$ cells were transfected with a siRNA against Fyn or a control siRNA. Lysates from control and transfected cells were immunoblotted with a βDG antibody. The histogram on the bottom panel shows the ratios cleaved βDG (30 kDa)/total βDG (43kDa). (**e**) Cell lysates from neurospheres derived from 129/ola or Prnp$^{0/0}$ mice, and either mock-infected or infected with 22L prions were immunoblotted with antibodies targeting βDG to calculate the ratio cleaved βDG (30 kDa)/total βDG (43 kDa; histogram, bottom panel). Results are expressed as means ± S.E.M of three independent experiments. *$P \leq 0.01$ and **$P \leq 0.05$ *versus* control (Student's *t*-test)

Finally, although the ratio cleaved βDG/total βDG was not affected in PrP$^{-/-}$ neurospheres exposed to the prion inoculum, PrP^{Sc} accumulation was associated with a 40% reduction in βDG cleavage in wild-type neurospheres at 5 d.p.i. (Figure 4e). Thus, the changes imparted by prion replication in differentiated wild-type neurospheres compare those observed in 1C11Fk$^{5\text{-HT}}$-infected cells.

Prion-induced impairment of MMP-9 activity causes imbalance between A-beta production and clearance. Another notable substrate of MMP-9 is the A-beta peptide,[18,19] whose accumulation because of overproduction or underclearance in the central nervous system causes Alzheimer's disease.[20] We thus wondered whether the reduction in MMP-9 activity evidenced in prion-infected cells would impact on the levels of extracellular A-beta. ELISA-based quantification of A-beta40 and A-beta42 in the supernatants of 1C11Fk$^{5\text{-HT}}$-infected cells revealed increased levels as compared with uninfected 1C11$^{5\text{-HT}}$ cells (Figure 5a and b). The impact of prion infection on extracellular A-beta levels was more drastic with 1C11Fk6$^{5\text{-HT}}$ than 1C11Fk7$^{5\text{-HT}}$ cells (Figure 5a and b). Of note, exposure of non-infected 1C11$^{5\text{-HT}}$ cells to MMP-9i (3 h, 5 nM), an inhibitor of MMP-9, led to increased extracellular A-beta40 and A-beta42 levels, indicating that the A-beta peptide indeed is a substrate of MMP-9 in 1C11$^{5\text{-HT}}$ cells (Figures 5c and d).

Next, we assessed the production and clearance rates of A-beta by incubating cells with $^{13}C_6$-Leucine for 3 h and collecting the supernatants over a 12-h time window. A-beta40 and A-beta42 levels were quantified through stable isotope labeling tandem mass spectrometry as in Bateman *et al.*[21] In uninfected 1C11$^{5\text{-HT}}$ cells, the production rate of A-beta was slightly lower than that of elimination, because we measured clearance rates of 0.948 and 0.951 for A-beta40 and A-beta42, respectively (Figure 6a and b). We next quantified the production and elimination of A-beta in 1C11Fk$^{5\text{-HT}}$-infected cells. As shown in Figure 6a

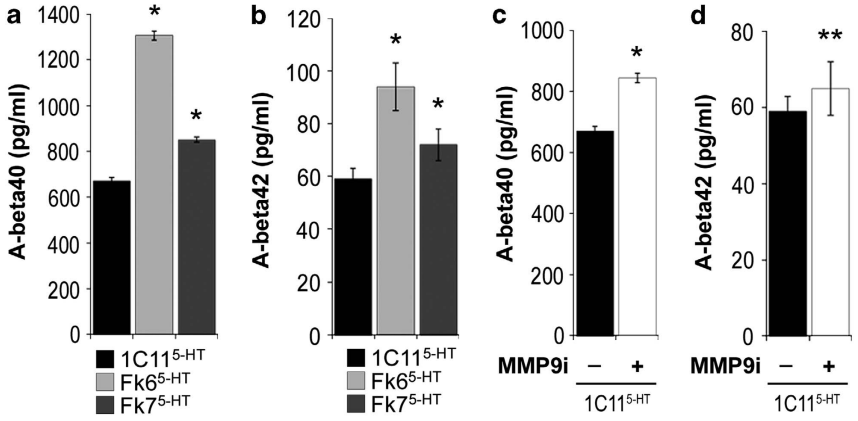


Figure 5 MMP-9 inhibition and prion infection increase extracellular A-beta levels *in vitro*. The steady-state levels of A-beta40 (**a**) and A-beta42 (**b**) were quantified in the supernatants of 1C11$^{5\text{-HT}}$ cells and their prion-infected counterparts, 1C11Fk6$^{5\text{-HT}}$ and 1C11Fk7$^{5\text{-HT}}$ cells. The contribution of MMP-9 to A-beta40 (**c**) and A-beta42 (**d**) elimination was assessed by exposing 1C11$^{5\text{-HT}}$-uninfected cells to the MMP-9 inhibitor MMP-9i. Data are presented as means ± S.E.M. of $n = 7$ independent measures. Values were evaluated by Student's *t*-test (*$P < 0.01$ and **$P \leq 0.05$ *versus* 1C11$^{5\text{-HT}}$ basal values)

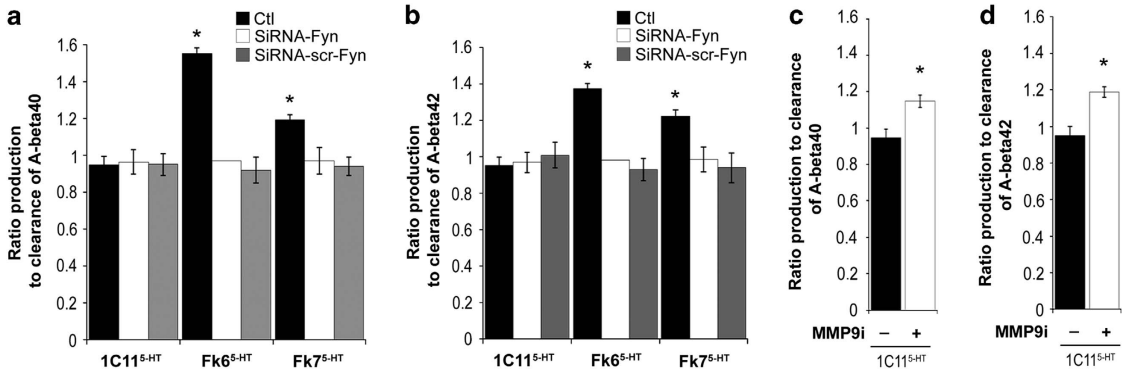


Figure 6 MMP-9 inhibition and prion infection impair A-beta clearance *in vitro*. The production and the clearance of A-beta40 (**a**) and A-beta42 (**b**) were measured in the supernatants of uninfected 1C11$^{5\text{-HT}}$ cells and the PrP^{Sc}-positive 1C11Fk6$^{5\text{-HT}}$ and 1C11Fk7$^{5\text{-HT}}$ cells. The contribution of the Fyn kinase to A-beta clearance was assessed through cell transfection with a siRNA targeting Fyn or a control siRNA. The involvement of MMP-9 in the elimination of A-beta40 (**c**) and A-beta42 (**d**) was evaluated by exposing 1C11$^{5\text{-HT}}$-uninfected cells to the MMP-9 inhibitor MMP-9i. Each value corresponds to the ratio production to clearance. Data are presented as means ± S.E.M. of $n = 6$–8 independent measures. Values were evaluated by Student's *t*-test (*$P < 0.01$ *versus* 1C11$^{5\text{-HT}}$ basal values)

and b, there were imbalances in the A-beta40 and A-beta42 production to clearance ratios, which were more pronounced in 1C11Fk6$^{5\text{-HT}}$ cells than in 1C11Fk7$^{5\text{-HT}}$ cells. Of note, when the same experiment was carried out in cells exposed to Fyn siRNA, the impact of PrP^{Sc} accumulation on the clearance rates of A-beta40 and A-beta42 was abrogated (Figure 6a and b). Finally, in 1C11$^{5\text{-HT}}$ cells, MMP-9 indeed contributes to the elimination of A-beta, because exposure of 1C11$^{5\text{-HT}}$ cells to MMP-9i (3 h, 5 nM) impaired the clearance of both A-beta40 and A-beta42 (Figure 6c and d), in line with the ELISA-based quantification (Figure 5c and d).

Thus, in 1C11Fk$^{5\text{-HT}}$-infected cells, the downregulation of MMP-9 activity resulting from the constitutive activation of PrP^{C}-related signaling cascades leads to impaired A-beta elimination.

A-beta levels are increased in the CSF of mice inoculated with 1C11Fk cells. Finally, we sought to extend these *in vitro* observations to the *in vivo* situation by quantifying A-beta40 and A-beta42 in the CSF of C57Bl/6J mice through ELISA. C57Bl/6J mice were inoculated with 1C11Fk6 or 1C11Fk7 cells and their CSF were collected at 150 d.p.i., that is, at a stage when mice start developing clinical signs. In mock-infected mice, the CSF levels of A-beta40 and A-beta42 reached 4754 and 526 pg/ml, respectively (Figure 7a and b). Of note, there was a 1.5-fold increase in the levels of both A-beta40 and A-beta42 in the CSF of mice inoculated with 1C11Fk6 cells, as compared with mock-infected mice (Figure 7a and b). We also measured a significant increase in the levels of both peptides in the CSF of mice inoculated with 1C11Fk7 cells, albeit to a milder extent (Figure 7a and b). Finally, we checked that MMP-9 contributes to the clearance of A-beta *in vivo*. In mock-infected mice treated with the MMP-9 inhibitor MMP-9i (500 ng, intraperitoneal injections twice a day) for 10 days, CSF A-beta40 and A-beta42 levels indeed increased by 1.2- and 1.25-fold, respectively, as compared with control mice (Figure 7c and d). These data are in line with *in vivo* observations showing high levels of A-beta42 in the CSF of sporadic CJD patients.[22] They provide further evidence that MMP-9 takes part to the degradation of A-beta[18,19] and argue that impaired activity of MMP-9 because of the deviation of PrP^{C} normal signaling function contributes to imbalances in A-beta clearance in the context of prion infection.

Discussion

A growing body of evidence argues that PrP^{Sc} exerts its neurotoxic action through the corruption of PrP^{C} normal function.[4,7] One hypothesis assumes that prion-associated neurodegeneration could result from the loss of PrP^{C} neuroprotective function upon its conversion into PrP^{Sc}. On another hand, it is proposed that the interaction of PrP^{Sc} with PrP^{C} could trigger a toxic gain of PrP^{C} function. In this study, we build upon our previous identification of downstream effectors of PrP^{C} signaling to shed light on the molecular outcome of PrP^{Sc} accumulation. Our results draw a link between PrP^{Sc}-associated intracellular events and PrP^{C}-coupled signaling pathways (Supplementary Figure S3). We show that, in both 1C11$^{5\text{-HT}}$ neuronal cells and differentiated wild-type neurospheres, prion infection is associated with the constitutive activation of several PrP^{C} proximal targets, including the Fyn kinase, ERK1/2 MAP kinases, the CREB transcription factor and its target gene Egr-1. Our data have to be brought together with *in vivo* observations, showing increased activities of Src kinases,[23] MAP kinases[24,25] and CREB[25] in the brains of scrapie-infected mice.

Downstream from the Fyn–ERK–CREB cascade, we further monitor a strong downregulation of MMP-9 in prion-infected cells, both at the level of mRNA and enzymatic activity. A direct consequence of this change is the decrease in the cleavage of the βDG when cells accumulate PrP^{Sc}. As MMP-9 has a critical role in synaptic activity and memory,[26] notably through the cleavage of the βDG,[27] the PrP^{Sc}-dependent blockade of MMP-9 may account for the cognitive and neurophysiological dysfunctions observed in scrapie-infected mice.[28]

Another dramatic outcome of the prion-induced reduction of MMP-9 activity is the impairment of A-beta clearance. Several links between PrP and A-beta have been recently disclosed,

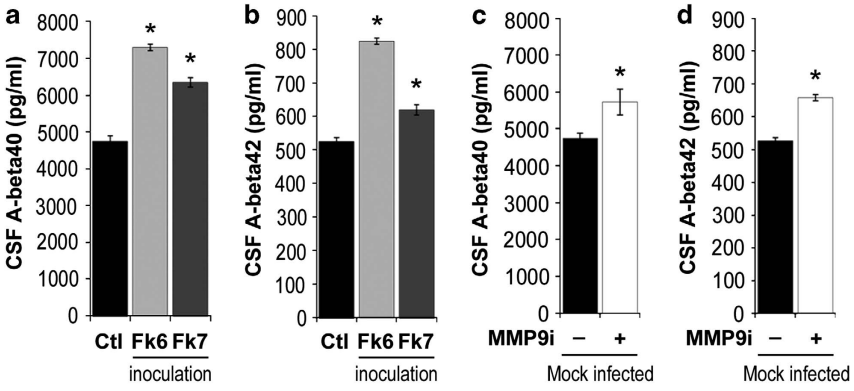


Figure 7 MMP-9 inhibition and prion infection increase A-beta levels in mouse CSF. The levels of A-beta40 (**a**) and A-beta42 (**b**) were measured in the CSF from mock-infected mice or mice infected with 1C11Fk6 or 1C11Fk7 cells. The contribution of MMP-9 to A-beta40 (**c**) and A-beta42 (**d**) elimination was assessed through a 10-day treatment with the MMP-9 inhibitor MMP-9i. Data are presented as means ± S.E.M. of $n = 5$–8 independent measures. Values were evaluated by Student's *t*-test ($^{*}P < 0.01$)

notably the – still debated – role of PrP^{C} as a receptor for A-beta.[29–31] PrP^{C} was also shown to protect against the generation of A-beta by sequestering the beta-secretase BACE1.[32] Our observation adds another level of complexity to the interplay between PrP and A-beta. The decrease in MMP-9 activity caused by pathogenic prions limits the degradation of A-beta. By promoting an accumulation of A-beta in the extracellular space, prion infection is likely to fuel a detrimental loop, further enhancing the interaction of A-beta with PrP^{Sc}.[33,34]

In line with the above idea, all the changes measured in this study, including the impairment in A-beta clearance, are more pronounced in 1C11Fk6$^{5\text{-HT}}$ cells than in 1C11Fk7$^{5\text{-HT}}$ cells, which accumulate less PrP^{Sc} and infectivity. The A-beta levels measured in the CSF of mice inoculated with infected cells are also higher with 1C11Fk6$^{5\text{-HT}}$ cells than 1C11Fk7$^{5\text{-HT}}$ cells. These observations are reminiscent of the dose-dependent prion-induced alterations of neurotransmitter-associated functions.[14] Notably, the activation of the SAPKs JNK and p38 appears to depend on a threshold level of PrP^{Sc} and infectivity because it is barely – if not – detected in the less infectious 1C11Fk7$^{5\text{-HT}}$ cells. These SAPKs are never recruited following antibody-mediated PrP^{C} ligation in the 1C11 cell line.[17] As observed after exposure of 1C11-derived neuronal cells to the prion peptide PrP106-126,[17] the activation of these SAPKs in 1C11Fk$^{5\text{-HT}}$ cells is strongly reduced on silencing of Fyn or NADPH oxidase. Thus, we propose that oxidative stress, a well-characterized feature of TSEs,[35] may originate from a deviation of the coupling of PrP^{C} to NADPH oxidase downstream from the Fyn kinase, and subsequently lead to the activation of cellular stress mediators.

An important contribution of this study is the connection of the molecular changes observed in prion-infected cells to the normal signaling function of PrP^{C}. PrP^{C} exerts a neurospecific role through the mobilization of a caveolin-Fyn platform.[7] A critical issue is how to relate transiently active signaling pathways with sustained changes evoked by permanent alterations in prion proteins. Within a physiological context, the downstream effectors of PrP^{C} signaling are transiently activated.[12,13] In contrast, we monitor here, in 1C11Fk$^{5\text{-HT}}$ chronically infected cells, a permanent activation (i.e., 'activated' state) of the targets of the PrP–caveolin–Fyn platform, including, at a proximal level, ERK and CREB. Fyn drives the steady-state changes leading to the 'constitutively activated' state observed in infected cells, because they are canceled under siRNA-mediated silencing of the Fyn kinase. Thus, there is a permanent recruitment of this kinase in the context of chronic prion replication. This directs the downstream activation of ERK and CREB, as well as the downregulation of MMP-9 and the impaired clearance of A-beta. From a mechanistic point of view, how can pathogenic prions trigger a sustained activation of the Fyn kinase? In non-infected 1C11$^{5\text{-HT}}$ neuronal cells, Fyn is transiently recruited by PrP^{C} molecules located in cholesterol-enriched rafts at the neurites.[7] Of note, lipid rafts are known to have a key part in prion neuropathogenesis (reviewed in Lewis and Hooper[36]). For instance, PrP^{Sc} accumulation promotes an increase in the level of free cholesterol,[37] and is associated with a reduction in membrane fluidity,[38] which may amplify the duration and/or strength of signaling.[39] In line with this, treatments with drugs disrupting the stability of lipid rafts reduce the toxicity of PrP^{Sc} *in vitro*[40] and prolong survival time in scrapie-infected mice.[41] Finally, a series of data exemplify a corruption of PrP^{C}-dependent pathway by PrP^{Sc}[42] or other beta-sheet conformers,[8,33,43] leading to neurotoxicity. Thus, we propose that prion infection triggers a durable aggregation of the PrP–caveolin–Fyn signaling platform within lipid rafts, with PrP^{C} being replaced by its pathogenic PrP^{Sc} isoform.

To summarize, our *in vitro* findings now introduce impaired A-beta clearance as a further consequence of the subversion of PrP^{C}-related signaling cascades by pathogenic prions. The relevance of this observation is substantiated by the elevated A-beta levels measured in the CSF of mice inoculated with 1C11Fk cells. Of note, A-beta was recently shown to enhance the clustering of PrP^{C} at the cell surface of neuronal cells,[44] and to cause neuronal impairment by activating Fyn via PrP^{C}.[45] Thus, the accumulation of A-beta in the environment of infected neurons is likely to sustain a vicious circle with an exacerbation of the constitutive recruitment of PrP-dependent signaling targets upon interaction of A-beta with PrP^{Sc} and further impairment in A-beta clearance. Achieving an integrated view of the signaling pathways sustaining the neurotoxicity of prions may have broad implications for designing therapeutic strategies to alleviate amyloid-associated neurodegeneration.

Materials and Methods

Material. All tissue culture reagents were from Invitrogen (Carlsbad, CA, USA). The anti-PrP monoclonal mouse antibody Sha31 was a kind gift of Dr. Jacques Grassi (CEA, Saclay, France). Polyclonal rabbit IgG antibodies against pan CREB and phospho-Ser133 CREB were purchased from Upstate Biotechnology (Lake Placid, NY, USA). Polyclonal rabbit antibodies against phospho-Tyr418 Src, pan Erk1/2, phospho-Thr185/Tyr187 Erk1/2, phospho-Thr183/Tyr185 JNK1/2 and phospho-Thr180/Tyr182 p38 were from Invitrogen. Polyclonal rabbit antibodies against pan src and monoclonal rabbit antibodies against Egr-1 and c-fos were from Cell Signaling Technology (Danvers, MA, USA). Monoclonal mouse antibody against βDG was purchased from Novocastra Laboratories Ltd (Newcastle, UK). Monoclonal mouse antibody against actin was from Novus Biologicals (Littleton, CO, USA). Proteinase K was from Roche (Penzberg, Germany). MMP-9i was from Calbiochem (San Diego, CA, USA). Dibutyryl cyclic AMP (dbcAMP), cyclohexane carboxylic acid (CCA), PMSF and DAPI were purchased from Sigma (St. Louis, MO, USA) and $^{13}C_6$-Leucine from Cambridge Isotope Laboratories (Andover, MA, USA).

1C11 cell culture and small interfering RNA transfection. 1C11 precursor and 1C11Fk-infected cells were grown and induced to differentiate along the serotonergic pathway in the presence of 1 mM dbcAMP and 0.05% CCA as in Mouillet-Richard *et al.*[10] Biolistic transfection of siRNA against Fyn (sc-35425 from Santa-Cruz, Santa Cruz, CA, USA), p22phox (sc-61892, Santa-Cruz) or control siRNAs (Santa Cruz), was carried out with a Helios Gene Gun (Bio-Rad, Hercules, CA, USA), according to the manufacturer's protocol. Transfection rates averaged 80%.

Isolation and prion infection of neurospheres. Mouse neurospheres were cultured as previously described in Herva *et al.*[15] Briefly, neurospheres were obtained by whole-brain dissection of 14-day embryo from two mouse lines: wild-type 129/ola and Prnp0/0 mice homozygous for a targeted null mutation in the PrP gene.[46] Cells were plated in N2 medium supplemented with 20 ng/ml basic fibroblast growth factor and 20 ng/ml epidermal growth factor. Neurospheres were seeded on coated plates to obtain a monolayer culture. At 80–90% of confluence, differentiation was induced by growth factor withdrawal in neurobasal B27 medium. The culture medium was replaced by the differentiation medium in combination with 22L prion or healthy (control) mouse inocula (1 : 50 from 10% brain homogenate stock, prepared in 5% glucose). After 24 h of incubation in the presence of the inocula, the culture was rinsed and fresh differentiation medium

was added. The culture medium was then changed every 2 days and at day 5 post-infection, cells were harvested in lysis buffer.

Immunofluorescence experiments. Cells were fixed in paraformaldehyde 3.7%, picric acid 0.15%, permeabilized with PBS containing 0.1% triton X-100, washed and blocked with PBS-0.2% BSA. Cells were incubated with antibodies against TujI (Covance, Princeton, NJ, USA) diluted 1 : 500 in PBS-0.2% BSA for 1 h at 37 °C. After incubation, cells were washed and incubated with secondary antibodies (Alexa fluor 594 goat anti-mouse IgG from Invitrogen, 1 : 7000) for 1 h at room temperature under light-shading conditions. After washing, cells were stained with DAPI for 5 min under agitation at room temperature and then rinsed with PBS and washed with H_2O. The slides were mounted with FluorSave Reagent (Calbiochem) and observed with Leica DMRA2 microscope (Wetzlar, Germany).

Preparation of cell extracts and western blot analyses. Uninfected 1C11$^{5\text{-HT}}$ or infected 1C11Fk$^{5\text{-HT}}$ cells and neurospheres were washed in PBS with 1 mM Ca^{2+} and Mg^{2+} and incubated for 30 min at 4 °C in NET lysis buffer (50 mM Tris · HCl (pH 7.4)/150 mM NaCl/5 mM EDTA/1% Triton X-100/1 mM Na_3VO_4 and a mixture of protease inhibitors, Roche, Mannheim, Germany). Extracts were centrifuged at 14 000 × *g* for 15 min. Protein concentrations in the supernatant were measured by using the bicinchoninic acid method (Pierce, Rockford, IL, USA). Ten micrograms of proteins were resolved by SDS/10% PAGE and transferred to nitrocellulose membranes (Amersham, Arlington Heights, IL, USA). Membranes were blocked with 0.5 gelatine and 0.5% goat serum or with 3% non-fat dry milk in PBS 0.1% Tween 20 for 1 h at room temperature and then incubated overnight at 4 °C with primary antibody (1 μg/ml). Bound antibody was revealed by enhanced chemiluminescence detection using a secondary antibody coupled to HRP (Amersham).

PrP^{res} detection. Cell lysates containing 80 μg of total proteins in 500 μl were digested with 10 μg/ml Proteinase K at 37 °C for 30 min. Digestion was terminated by the addition of PMSF to 1 mM and samples were centrifuged at 14 000 × *g*, 4 °C, for 1 h. Pellets were resuspended in 15 μl of sample buffer, boiled 10 min at 100 °C and analyzed by western blot using Sha31 antibody.

Zymography. Twenty microliter of the culture medium were loaded on 10% Tris-Glycine gels containing 0.1% gelatin. After electrophoresis, gels were incubated in Novex Zymogram Renaturing Buffer (Invitrogen) for 30 min at room temperature with gentle agitation. Gels were then equilibrated in Novex Zymogram Developing buffer (Invitrogen) for 30 min at room temperature with gentle agitation. Gels were then incubated overnight at 37 °C in fresh developing buffer and stained with SimplyBlue SafeStain (Invitrogen) for 1 h at room temperature with gentle agitation. The protease bands appear as clear bands against a dark background.

Isolation of total RNA and reverse transcriptase (RT)-PCR. RNA was isolated by using RNase Easy Kit from Qiagen (Hilden, Germany) including a RNase-free DNase I digestion step, as recommended by the manufacturer's instructions. For RT-PCR analysis, first-strand cDNA was synthesized from with oligo(dT)$_{12\text{-}18}$ primer, using 400 units of Superscript III reverse transcriptase (Invitrogen) according to the manufacturer's protocol. PCR amplifications were then carried out in a 50 μl volume containing 1 μl of the reverse transcription products, using Taq DNA polymerase (Invitrogen). PCR products were analyzed on 2% agarose gels. Primers used for the PCR reactions include: GAPDH forward 5′-TGAAGGTCGGTGTGAACGGAT-3′ and reverse 5′-CATGTAGGCCATGAG GTCCAC-3′; Egr-1 forward 5′-AAGACACCCCCCCATGAAC-3′ and reverse 5′-GC GAGAAAAGCGGCGAT-3′; c-Fos forward 5′-ACGGAGAATCCGAAGGGAACGG AATAAATGGC-3′ and reverse 5′-GACAAAGGAAGACGTGTAAGTAGTGCAGC-3′; MMP-9 forward 5′-CCATGAGTCCCTGGCAG-3′ and reverse 5′-AGTATGTGATG TTATGATG-3.

Measurements of A-beta production and clearance. 1C11$^{5\text{-HT}}$ cells and their infected counterparts were incubated with $^{13}C_6$-Leucine (98% $^{13}C_6$) in OptiMEM medium for 3 h. Pulse medium was then replaced by fresh OptiMEM and supernatants were collected over a 12 h time window. A-beta42 and then A-beta40 were serially immunoprecipitated from the samples using C-terminal-specific antibodies, (NB300-225 from Novus Biologicals and ABIN363343 from Antibodies online, Atlanta, GA, USA). Purified A-beta peptides were then digested with trypsin and $^{13}C_6$-leucine abundance in these tryptic fragments quantified using tandem mass spectrometry as previously described.[21]

Mouse CSF collection. Animal experiments were carried out in strict accordance with the recommendations in the guidelines of the Code for Methods and Welfare Considerations in Behavioral Research with Animals (Directive 86/609EC) and all efforts were made to minimize suffering. Experiments were approved by the Committee on the Ethics of Animal Experiments of Basel University. Ten 8-week-old male C57BL/6J mice per group were inoculated intracerebrally with 20 μl of sample containing cell extracts (2.10^6 cells) as in Mouillet-Richard *et al.*[14] Cells were submitted to three freeze–thaw cycles and suspensions were sonicated for 2 min (Cup-horn sonicator; Nanolab Inc, Waltham, MA, USA). CSF was collected at 150 d.p.i. (i.e., clinical stage) from cisterna magna and frozen at − 80 °C.

Measurement of A-beta levels. A-beta40 and A-beta42 were quantified in cell supernatant or CSF through ELISA (My Biosource MBS494458 and MBS704748, San Diego, CA, USA).

Statistics. Protein and mRNA levels were quantified using NIH ImageJ software (http://rsb.info.nih.gov/ij/). Statistical analysis to determine significance used the unpaired Student's *t*-test while error bars on all graphs represent the S.E.M. A P-value < 0.05 was considered significant.

Conflict of Interest

The authors declare no conflict of interest.

Acknowledgements. We thank J Grassi for his kind gift of Sha31 antibody. We gratefully acknowledge the mass spec team of Z Lam for skillful methodological assistance, V Mutel and A Baudry for critical reading of the manuscript. This work was supported by funds from the Agence Nationale de la Recherche (ANR-06-BLAN-0288 and ANR-10-BLANC-131201) and INSERM (OK) and a EU grant (PRIORITY CT2009-222887, JMT). EP was supported by a Neuroprion Start-up grant and a fellowship from the Fondation de la Recherche Medicale. OK is a professor at the Université Paris Sud.

1. Aguzzi A, Calella AM. Prions: protein aggregation and infectious diseases. *Physiol Rev* 2009; **89**: 1105–1152.
2. Mallucci G, Dickinson A, Linehan J, Klohn PC, Brandner S, Collinge J. Depleting neuronal PrP in prion infection prevents disease and reverses spongiosis. *Science* 2003; **302**: 871–874.
3. Chesebro B, Trifilo M, Race R, Meade-White K, Teng C, LaCasse R *et al.* Anchorless prion protein results in infectious amyloid disease without clinical scrapie. *Science* 2005; **308**: 1435–1439.
4. Westergard L, Christensen HM, Harris DA. The cellular prion protein (PrP(C)): its physiological function and role in disease. *Biochim Biophys Acta* 2007; **1772**: 629–644.
5. Bueler H, Aguzzi A, Sailer A, Greiner RA, Autenried P, Aguet M *et al.* Mice devoid of PrP are resistant to scrapie. *Cell* 1993; **73**: 1339–1347.
6. Chiesa R, Piccardo P, Biasini E, Ghetti B, Harris DA. Aggregated, wild-type prion protein causes neurological dysfunction and synaptic abnormalities. *J Neurosci* 2008; **28**: 13258–13267.
7. Schneider B, Pietri M, Pradines E, Loubet D, Launay JM, Kellermann O *et al.* Understanding the neurospecificity of prion protein signaling. *Front Biosci* 2011; **16**: 169–186.
8. Resenberger UK, Harmeier A, Woerner AC, Goodman JL, Muller V, Krishnan R *et al.* The cellular prion protein mediates neurotoxic signalling of beta-sheet-rich conformers independent of prion replication. *EMBO J* 2011; **30**: 2057–2070.
9. Linden R, Martins VR, Prado MA, Cammarota M, Izquierdo I, Brentani RR. Physiology of the prion protein. *Physiol Rev* 2008; **88**: 673–728.
10. Mouillet-Richard S, Mutel V, Loric S, Tournois C, Launay JM, Kellermann O. Regulation by neurotransmitter receptors of serotonergic or catecholaminergic neuronal cell differentiation. *J Biol Chem* 2000; **275**: 9186–9192.
11. Mouillet-Richard S, Ermonval M, Chebassier C, Laplanche JL, Lehmann S, Launay JM *et al.* Signal transduction through prion protein. *Science* 2000; **289**: 1925–1928.
12. Pradines E, Loubet D, Schneider B, Launay JM, Kellermann O, Mouillet-Richard S. CREB-dependent gene regulation by prion protein: impact on MMP-9 and beta-dystroglycan. *Cell Signal* 2008; **20**: 2050–2058.
13. Schneider B, Mutel V, Pietri M, Ermonval M, Mouillet-Richard S, Kellermann O. NADPH oxidase and extracellular regulated kinases 1/2 are targets of prion protein signaling in neuronal and nonneuronal cells. *Proc Natl Acad Sci USA* 2003; **100**: 13326–13331.
14. Mouillet-Richard S, Nishida N, Pradines E, Laude H, Schneider B, Feraudet C *et al.* Prions impair bioaminergic functions through serotonin- or catecholamine-derived neurotoxins in neuronal cells. *J Biol Chem* 2008; **283**: 23782–23790.

15. Herva ME, Relano-Gines A, Villa A, Torres JM. Prion infection of differentiated neurospheres. *J Neurosci Methods* 2010; **188**: 270–275.
16. Lam BY, Zhang W, Enticknap N, Haggis E, Cader MZ, Chawla S. Inverse regulation of plasticity-related immediate early genes by calcineurin in hippocampal neurons. *J Biol Chem* 2009; **284**: 12562–12571.
17. Pietri M, Caprini A, Mouillet-Richard S, Pradines E, Ermonval M, Grassi J *et al.* Overstimulation of PrPC signaling pathways by prion peptide 106-126 causes oxidative injury of bioaminergic neuronal cells. *J Biol Chem* 2006; **281**: 28470–28479.
18. Merlo S, Sortino MA. Estrogen activates matrix metalloproteinases-2 and -9 to increase beta amyloid degradation. *Mol Cell Neurosci* 2012; **49**: 423–429.
19. Yan P, Hu X, Song H, Yin K, Bateman RJ, Cirrito JR *et al.* Matrix metalloproteinase-9 degrades amyloid-beta fibrils *in vitro* and compact plaques in situ. *J Biol Chem* 2006; **281**: 24566–24574.
20. Haass C, Selkoe DJ. Soluble protein oligomers in neurodegeneration: lessons from the Alzheimer's amyloid beta-peptide. *Nat Rev Mol Cell Biol* 2007; **8**: 101–112.
21. Bateman RJ, Munsell LY, Chen X, Holtzman DM, Yarasheski KE. Stable isotope labeling tandem mass spectrometry (SILT) to quantify protein production and clearance rates. *J Am Soc Mass Spectrom* 2007; **18**: 997–1006.
22. Zanusso G, Fiorini M, Ferrari S, Gajofatto A, Cagnin A, Galassi A *et al.* Cerebrospinal fluid markers in sporadic Creutzfeldt-Jakob disease. *Int J Mol Sci* 2011; **12**: 6281–6292.
23. Nixon RR. Prion-associated increases in Src-family kinases. *J Biol Chem* 2005; **280**: 2455–2462.
24. LaCasse RA, Striebel JF, Favara C, Kercher L, Chesebro B. Role of Erk1/2 activation in prion disease pathogenesis: absence of CCR1 leads to increased Erk1/2 activation and accelerated disease progression. *J Neuroimmunol* 2008; **196**: 16–26.
25. Lee HP, Jun YC, Choi JK, Kim JI, Carp RI, Kim YS. Activation of mitogen-activated protein kinases in hamster brains infected with 263K scrapie agent. *J Neurochem* 2005; **95**: 584–593.
26. Rivera S, Khrestchatisky M, Kaczmarek L, Rosenberg GA, Jaworski DM. Metzincin proteases and their inhibitors: foes or friends in nervous system physiology? *J Neurosci* 2010; **30**: 15337–15357.
27. Michaluk P, Kolodziej L, Mioduszewska B, Wilczynski GM, Dzwonek J, Jaworski J *et al.* Beta-dystroglycan as a target for MMP-9, in response to enhanced neuronal activity. *J Biol Chem* 2007; **282**: 16036–16041.
28. Mallucci GR, White MD, Farmer M, Dickinson A, Khatun H, Powell AD *et al.* Targeting cellular prion protein reverses early cognitive deficits and neurophysiological dysfunction in prion-infected mice. *Neuron* 2007; **53**: 325–335.
29. Benilova I, De Strooper B. Prion protein in Alzheimer's pathogenesis: a hot and controversial issue. *EMBO Mol Med* 2010; **2**: 289–290.
30. Gunther EC, Strittmatter SM. Beta-amyloid oligomers and cellular prion protein in Alzheimer's disease. *J Mol Med* 2010; **88**: 331–338.
31. Kellett KA, Hooper NM. Prion protein and Alzheimer disease. *Prion* 2009; **3**: 190–194.
32. Griffiths HH, Whitehouse IJ, Baybutt H, Brown D, Kellett KA, Jackson CD *et al.* Prion protein interacts with BACE1 protein and differentially regulates its activity toward wild type and Swedish mutant amyloid precursor protein. *J Biol Chem* 2011; **286**: 33489–33500.
33. Resenberger UK, Winklhofer KF, Tatzelt J. Neuroprotective and neurotoxic signaling by the prion protein. *Top Curr Chem* 2011; **305**: 101–119.
34. Zou WQ, Xiao X, Yuan J, Puoti G, Fujioka H, Wang X *et al.* Amyloid-beta42 interacts mainly with insoluble prion protein in the Alzheimer brain. *J Biol Chem* 2011; **286**: 15095–15105.
35. Singh N, Singh A, Das D, Mohan ML. Redox control of prion and disease pathogenesis. *Antioxid Redox Signal* 2010; **12**: 1271–1294.
36. Lewis V, Hooper NM. The role of lipid rafts in prion protein biology. *Front Biosci* 2011; **16**: 151–168.
37. Bate C, Tayebi M, Williams A. Sequestration of free cholesterol in cell membranes by prions correlates with cytoplasmic phospholipase A2 activation. *BMC Biol* 2008; **6**: 8.
38. Wong K, Qiu Y, Hyun W, Nixon R, VanCleff J, Sanchez-Salazar J *et al.* Decreased receptor-mediated calcium response in prion-infected cells correlates with decreased membrane fluidity and IP3 release. *Neurology* 1996; **47**: 741–750.
39. Golub T, Wacha S, Caroni P. Spatial and temporal control of signaling through lipid rafts. *Curr Opin Neurobiol* 2004; **14**: 542–550.
40. Gilch S, Bach C, Lutzny G, Vorberg I, Schatzl HM. Inhibition of cholesterol recycling impairs cellular PrP(Sc) propagation. *Cell Mol Life Sci* 2009; **66**: 3979–3991.
41. Vetrugno V, Di Bari MA, Nonno R, Puopolo M, D'Agostino C, Pirisinu L *et al.* Oral pravastatin prolongs survival time of scrapie-infected mice. *J Gen Virol* 2009; **90**(Pt 7): 1775–1780.
42. Rambold AS, Muller V, Ron U, Ben-Tal N, Winklhofer KF, Tatzelt J. Stress-protective signalling of prion protein is corrupted by scrapie prions. *EMBO J* 2008; **27**: 1974–1984.
43. Bate C, Williams A. Amyloid-beta-induced synapse damage is mediated via cross-linkage of cellular prion proteins. *J Biol Chem* 2011; **286**: 37955–37963.
44. Caetano FA, Beraldo FH, Hajj GN, Guimaraes AL, Jurgensen S, Wasilewska-Sampaio AP *et al.* Amyloid-beta oligomers increase the localization of prion protein at the cell surface. *J Neurochem* 2011; **117**: 538–553.
45. Um JW, Nygaard HB, Heiss JK, Kostylev MA, Stagi M, Vortmeyer A *et al.* Alzheimer amyloid-beta oligomer bound to postsynaptic prion protein activates Fyn to impair neurons. *Nat Neurosci* 2012; **15**: 1227–1235.
46. Manson JC, Clarke AR, Hooper ML, Aitchison L, McConnell I, Hope J. 129/Ola mice carrying a null mutation in PrP that abolishes mRNA production are developmentally normal. *Mol Neurobiol* 1994; **8**: 121–127.

SOME RIGHTS RESERVED

Cell Death and Disease **is an open-access journal published by** ***Nature Publishing Group*****. This work is licensed under the Creative Commons Attribution-NonCommercial-No Derivative Works 3.0 Unported License. To view a copy of this license, visit http://creativecommons.org/licenses/by-nc-nd/3.0/**

Supplementary Information accompanies the paper on Cell Death and Disease website (http://www.nature.com/cddis)